Mineralogical Magazine (2022), **86**, 841–848
doi:10.1180/mgm.2022.65

CAMBRIDGE UNIVERSITY PRESS

Article

Kaznakhtite, $Ni_6Co_2^{3+}(CO_3)(OH)_{16}{\cdot}4H_2O$, a new natural layered double hydroxide, the member of the hydrotalcite supergroup

Anatoly V. Kasatkin[1]*, Sergey N. Britvin[2,3], Maria G. Krzhizhanovskaya[2], Nikita V. Chukanov[4], Radek Škoda[5], Jörg Göttlicher[6], Dmitry I. Belakovskiy[1], Igor V. Pekov[7] and Victor V. Levitskiy[1]

[1]Fersman Mineralogical Museum of the Russian Academy of Sciences, Leninsky Prospekt 18-2, 119071 Moscow, Russia; [2]St. Petersburg State University, University Emb. 7/9, 199034 St. Petersburg, Russia; [3]Nanomaterials Research Center, Kola Science Center of Russian Academy of Sciences, Fersman Str. 14, 184209 Apatity, Murmansk Region, Russia; [4]Institute of Problems of Chemical Physics of the Russian Academy of Sciences, 142432 Chernogolovka, Moscow region, Russia; [5]Department of Geological Sciences, Faculty of Science, Masaryk University, Kotlářská 2, 611 37, Brno, Czech Republic; [6]Karlsruhe Institute of Technology, Institute for Synchrotron Radiation, Hermann-von-Helmholtz-Platz 1, D-76344, Eggenstein-Leopoldshafen, Germany; and [7]Faculty of Geology, Moscow State University, Vorobievy Gory, 119991 Moscow, Russia

Abstract

Kaznakhtite, ideally $Ni_6Co_2^{3+}(CO_3)(OH)_{16}{\cdot}4H_2O$, is a new member of the hydrotalcite group within the hydrotalcite supergroup. The mineral was discovered at the Kaznakhtinskiy ultrabasic massif, Altai Republic, SW Siberia, Russia. It occurs as powdery aggregates forming flattened lenses up to 1.5 × 0.5 cm and veinlets up to 1 cm long and up to 1 mm thick in aggregates of chrysotile, lizardite, stichtite and dolomite. Other associated minerals include brucite, chromite, heazlewoodite, manganochromite, magnetite and magnesioferrite. Kaznakhtite aggregates are composed of tiny platy grains up to 0.01 mm across. Kaznakhtite is light green and translucent in aggregates. It has an earthy lustre and white streak. Cleavage is micaceous on {001}. D_{calc} = 2.864 g cm^{-3}. The mineral is optically uniaxial (–) with ε = 1.657(3) and ω = 1.676(3), and weakly pleochroic in greenish hues, ω > ε. Chemical composition (wt.%, electron microprobe, Co valence state determined by XANES spectroscopy, CO_2 and H_2O calculated by stoichiometry) is: MgO 2.15, NiO 47.40, ZnO 0.22, Al_2O_3 0.16, Cr_2O_3 0.98, Co_2O_3 17.42, Cl 0.63, CO_2 5.05, H_2O 24.60, –O=Cl –0.14, total 98.47. The empirical formula calculated based on the sum of all metal cations = 8 apfu is $(Ni_{5.54}Mg_{0.47}Zn_{0.02})_{\Sigma 6.03}(Co^{3+}_{1.83}Cr_{0.11}Al_{0.03})_{\Sigma 1.97}C_{1.00}O_{2.99}(OH)_{15.84}Cl_{0.16}{\cdot}4H_2O$. Infrared spectroscopy confirmed the presence of CO_3^{2-} anions, OH^- groups and H_2O molecules. The crystal structure was refined by the Rietveld method with R_B = 0.19%. Kaznakhtite is trigonal, space group $\overline{R}3m$, a = 3.0515 (3), c = 23.180 (3) Å, V = 186.93 (4) Å^3 and Z = 3/8. The strongest lines of the powder X-ray diffraction pattern [d, Å (I, %) (hkl)] are: 7.72 (100) (003); 3.863 (24) (006); 2.630 (4) (101); 2.576 (10) (012); 2.294 (6) (015); 1.950 (4) (018); 1.526 (4) (110); and 1.497 (4) (113). Kaznakhtite is a Co^{3+} analogue of reevesite, $Ni_6Fe_2^{3+}(CO_3)(OH)_{16}{\cdot}4H_2O$. The mineral is named after its type locality.

Keywords: kaznakhtite, new mineral, XANES, IR spectroscopy, crystal structure, hydrotalcite supergroup, layered double hydroxide, Kaznakhtinskiy ultrabasic massif, Altai Republic

(Received 5 March 2022; accepted 8 May 2022; Accepted Manuscript published online: 21 July 2022; Associate Editor: Elena Zhitova)

Introduction

The minerals of the hydrotalcite supergroup belong to a large family of layered double hydroxides (LDH) that comprises natural and synthetic compounds. The LDH crystal structure consists of alternating metal hydroxide layers formed by octahedra, in which cations of the metal M (uni-, di- or trivalent) are surrounded by OH groups, and a water–anion component that occupies the interlayer space (Rives, 2001; Evans and Slade, 2006; Britvin, 2008; Krivovichev *et al.*, 2012; Mills *et al.*, 2012a; Zhitova *et al.*, 2020). To date, the hydrotalcite supergroup includes 46 minerals. Fourty-three of them, including several questionable species, are mentioned in the most recent nomenclature report for the hydrotalcite supergroup (Mills *et al.*, 2012a). Since that time, four new species have been described [akopovaite (Karpenko *et al.*, 2020), dritsite (Zhitova *et al.*, 2019), erssonite (Zhitova *et al.*, 2021) and luidongshengite (Yang *et al.*, 2021)]; whereas jamborite was redefined as a mineral species which does not belong to the hydrotalcite supergroup (Bindi *et al.*, 2015). Here we report on a new member of the supergroup, kaznakhtite (pronounced kəz nah tait; Cyrillic – казнахтит), named after its type locality – Kaznakhtinskiy ultrabasic massif, Ust'-Koksinskiy District, Altai Republic, SW Siberia, Russia. On a lower hierarchical level kaznakhtite belongs to the hydrotalcite group (Mills *et al.*, 2012a), in which representatives typically have a 3 : 1 ratio of divalent and trivalent cations M^{2+} : M^{3+} in octahedral layers. For the case of kaznakhtite, Ni and Co are the species-defining divalent and trivalent cations, respectively, while CO_3^{2-} anion and water molecules occur in the interlayer space.

Both the new mineral and its name (symbol Kzt) have been approved by the Commission on New Minerals, Nomenclature

*Author for correspondence: Anatoly V. Kasatkin, Email: anatoly.kasatkin@gmail.com
Cite this article: Kasatkin A.V., Britvin S.N., Krzhizhanovskaya M.G., Chukanov N.V., Škoda R., Göttlicher J., Belakovskiy D.I., Pekov I.V. and Levitskiy V.V. (2022) Kaznakhtite, $Ni_6Co_2^{3+}(CO_3)(OH)_{16}{\cdot}4H_2O$, a new natural layered double hydroxide, the member of the hydrotalcite supergroup. *Mineralogical Magazine* **86**, 841–848. https://doi.org/10.1180/mgm.2022.65

and Classification of the International Mineralogical Association (IMA2021-056, Kasatkin *et al.*, 2021). The holotype specimen is deposited in the collections of the Fersman Mineralogical Museum of the Russian Academy of Sciences, Moscow, Russia with the registration number 5727/1.

Occurrence and mineral association

Specimens containing the new mineral were collected in July 2019 by one of the authors (V.V.L.) at the Kaznakhtinskiy ultrabasic massif, Ust'-Koksinskiy District, Altai Republic, SW Siberia, Russia. The exact locality (50°14'22"N, 86°30'25"E) is ~2 km to the west of the headwaters of the Kyzyl-Uyuk creek, the right tributary of the Kaznakhta river (Fig. 1).

The Kaznakhtinskiy ultrabasic massif is located at Terekta (Terektinskiy) Range which is a part of Russian Gorny Altai, on the watershed between the Kaznakhta river and Kyzyl-Uyuk and Kara-Uyuk creeks. It occupies an area up to 2 km long and 0.4 km across and represents a nearly vertical lens in shape accompanied by a series of small, steeply-inclined lenses (Kuznetsov, 1958). Geologically, the Kaznakhtinskiy massif is confined to the Kaznakhta ophiolite zone of the Terekta Ridge (northern branch of the Terekta ophiolite belt, Gorny Altai) and is associated with the thrust-sheet zone of the steep Charysh–Terekta deep fault. The Kaznakhta ophiolite body is composed of weakly metamorphosed volcanic–sedimentary rocks of the Baratal formation and various serpentinites. The northern part of the Kaznakhta ophiolite body is composed of chrysotile–lizardite serpentinites which contain inclusions of peridotites, shales, limestones, rodingites and rodingitised porphyrites. The southern zone of the body includes serpentinites of mostly antigorite composition, as well as dunites and granodiorites. The age of the serpentinites was determined as Carboniferous, and for some bodies it is presumably Cambrian. According to views on the tectonics of the Terekta Range region, in the early Cambrian and Carboniferous this was an area of complex subduction and collisional processes (Tatarinov *et al.*, 1985; Zhitova *et al.*, 2020).

The Kaznakhtinskiy massif is well known for occurrences of chromium-rich minerals of the hydrotalcite group, and is where stichtite was first found and is the most abundant. It composes ~5–20% of the volume (visual estimate) of chrysotile–lizardite serpentinites in the northern zone of the Kaznakhta ophiolite body (Tatarinov *et al.*, 1985; Rychkov and Rychkova, 2015; Zhitova *et al.*, 2020). Recently, woodallite, Cr-rich pyroaurite and Cr-rich iowaite have also been reported. They are characterised by large variations in chemical composition and, together with stichtite, here they form a complex solid-solution system (Zhitova *et al.*, 2020). Thus, kaznakhtite is the fifth member of the hydrotalcite group found at this locality.

Kaznakhtite is associated closely with chrysotile, lizardite, stichtite, dolomite, heazlewoodite, brucite and Cr-bearing minerals of the spinel group (chromite, manganochromite, Cr-rich magnetite and Cr-rich magnesioferrite).

General appearance and physical properties

Kaznakhtite occurs as very fine grained, powdery aggregates forming flattened lenses up to 1.5 cm × 0.5 cm and veinlets up to 1 cm long and up to 1 mm thick in altered ultramafic rock composed of chrysotile, lizardite, stichtite and dolomite. Kaznakhtite aggregates are composed of very tiny platy grains up to 0.01 mm across (Figs 2 and 3). The new mineral is light green, transparent in tiny grains and translucent in aggregates. It has an earthy lustre, white streak and laminated fracture. Its tenacity is not determined because of the earthy character of aggregates, however, by analogy with other hydrotalcite-group minerals, we could suggest that kaznakhtite particles are flexible and not elastic. The mineral has a micaceous cleavage on {001}. The hardness and density of kaznakhtite could not be determined because of the powdery nature of the mineral and its intimate intergrowths with chrysotile and lizardite. Density calculated using the empirical formula is 2.864 g cm^{-3}.

Kaznakhtite is optically uniaxial (–), with $\varepsilon = 1.657(3)$ and $\omega = 1.676(3)$ (589 nm). Under the microscope, it is marsh green in thicker grains to colourless in the thinnest grains and weakly pleochroic in greenish hues, $\omega > \varepsilon$. The Gladstone–Dale compatibility index (Mandarino, 1981) calculated based on the empirical formula is $1 - (K_p/K_c) = 0.059$ (good).

Fig. 1. Kaznakhtinskiy massif. The red arrow indicates the exact place where specimens with kaznakhtite were collected. Summer 2019. Photo: V.V. Mukhanov.

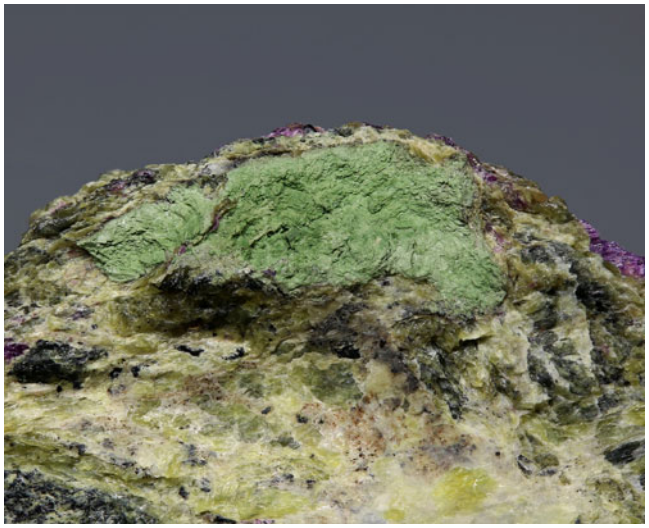

Fig. 2. Light green powdery kaznakhtite in fracture of serpentine (composed of intimately intergrown chrysotile and lizardite) with lilac stichtite. Fragment of holotype sample, Fersman Mineralogical Museum registration number 5727/1. Field of view: 3 × 2 cm.

https://doi.org/10.1180/mgm.2022.65 Published online by Cambridge University Press

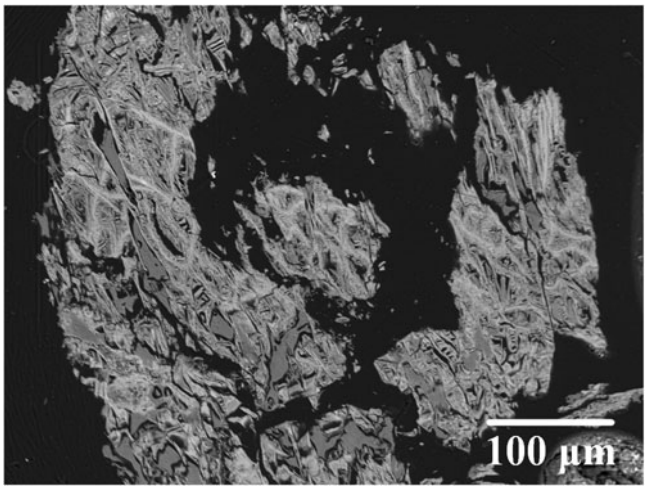

Fig. 3. Aggregates of kaznakhtite (white) in cracks of lizardite serpentinite (grey). Polished section. SEM (BSE) image.

Spectroscopical studies

Infrared spectroscopy

In order to obtain an infrared (IR) absorption spectrum, a powdered sample was mixed with anhydrous KBr, pelletised, and analysed using an ALPHA FTIR spectrometer (Bruker Optics) in the range of 360–3800 cm^{-1}, at a resolution of 4 cm^{-1}. A total of 16 scans were collected. The IR spectrum of an analogous pellet of pure KBr was used as a reference. The assignment of absorption bands in the IR spectrum of kaznakhtite (Fig. 4) is as follows.

Bands in the range of 3000–3600 cm^{-1} correspond to O–H stretching vibrations and the ones at 1572 and 1606 cm^{-1} to bending vibrations of H_2O molecules. The band at 1366 cm^{-1} is assigned to asymmetric stretching vibrations of CO_3^{2-} anions. Bands at 857 and 875 cm^{-1} are due to out-of-plane bending vibrations of CO_3^{2-} anions (nondegenerate mode) and those at 717 and 728 cm^{-1} to in-plane bending vibrations of CO_3^{2-} anions (degenerate mode). Numerous overlapping bands in the range 650–750 cm^{-1} correspond to librational modes of H_2O and OH^-. The bands at 533 cm^{-1} and 424 cm^{-1} are attributed to Co^{3+}–O and Ni^{2+}–O stretching vibrations, respectively.

X-ray absorption near-edge structure spectroscopy

In order to determine the valence state of Co in kaznakhtite, the Co *K*-edge X-ray absorption near-edge structure (XANES) spectra of the mineral and Co(II) and Co(III) reference substances have been measured at the SUL-x wiggler beamline of the synchrotron light source at the Karlsruhe Institute of Technology (KIT). Samples were prepared as pellets mixed with cellulose. Spectra were measured in transmission mode using ionisation chambers optimised with gas filling and pressure. A fixed exit Si(111) double crystal monochromator was used for tuning the energy across the absorption edge. The beam was collimated to ~800 µm × 800 µm at the sample position. Energy calibration was performed using the Co metal foil. Pre- and post-edge background subtraction and normalisation were done with *ATHENA* software in the *IFFEfit* package (Ravel and Newville, 2005).

The Co *K*-edge X-ray absorption edge of kaznakhtite is located at the typical energy of a $Co^{3+}OOH$ reference spectrum and is clearly separated from a $Co^{2+}(OH)_2$ reference spectrum with the

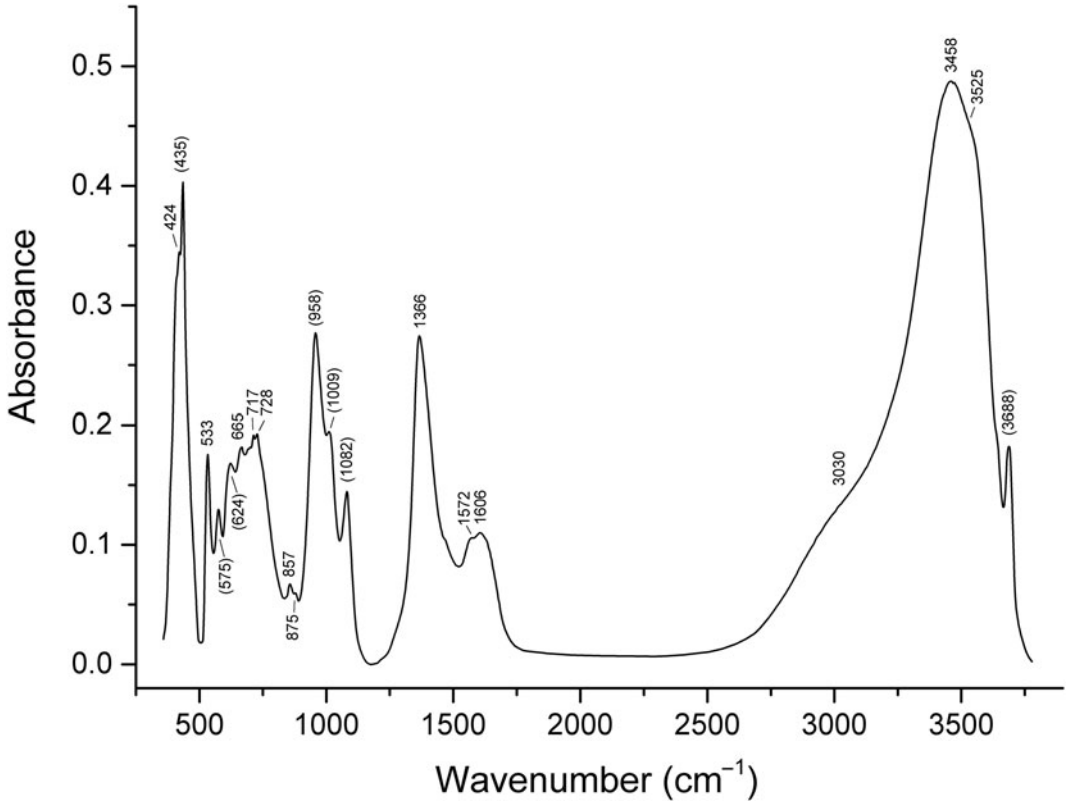

Fig. 4. Powder infrared absorption spectrum of kaznakhtite. Wavenumbers of admixed lizardite are given in parentheses.

https://doi.org/10.1180/mgm.2022.65 Published online by Cambridge University Press

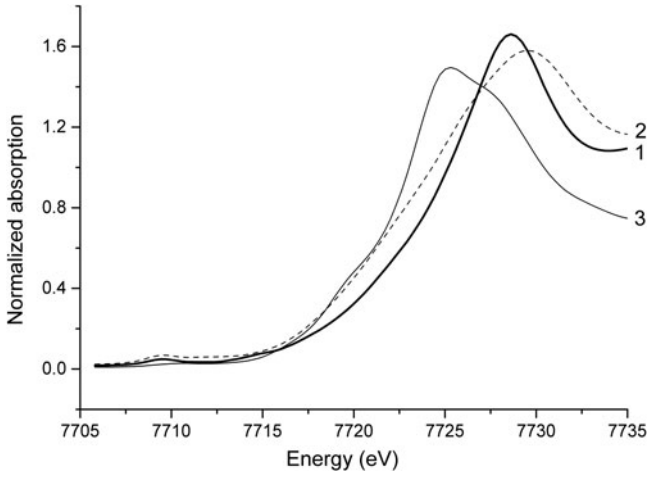

Fig. 5. Co *K*-edge XANES spectra of (1) kaznakhtite, (2) heterogenite $Co^{3+}OOH$ from the Democratic Republic of the Congo, and (3) synthetic $Co^{2+}(OH)_2$.

absorption edge of the latter at significantly lower energy (Fig. 5). A comparison of the kaznakhtite Co *K*-edge X-ray absorption spectrum with spectra of Co hydroxides and other reference substances (Fig. 6) confirms the conclusion on the trivalent state of cobalt in kaznakhtite.

Chemical composition and chemical properties

Sixteen electron-microprobe analyses were carried out with a Cameca SX-100 electron microprobe (wavelength dispersive spectroscopy mode with an accelerating voltage of 15 kV, a beam current on the specimen of 4 nA and a beam diameter of 10 μm). Peak counting times (CT) were 20 s for all elements; CT for each background was one-half of the peak time. The raw intensities were converted into concentrations using *X-PHI* (Merlet, 1994) matrix-correction software. H_2O and CO_2 were not determined directly because of the paucity of pure material. The presence of CO_3^{2-} anions, OH^- groups and H_2O molecules as species-defining constituents in kaznakhtite is shown conclusively by the structure and IR spectroscopy data. The presence of CO_3^{2-} is also confirmed by chemical test.

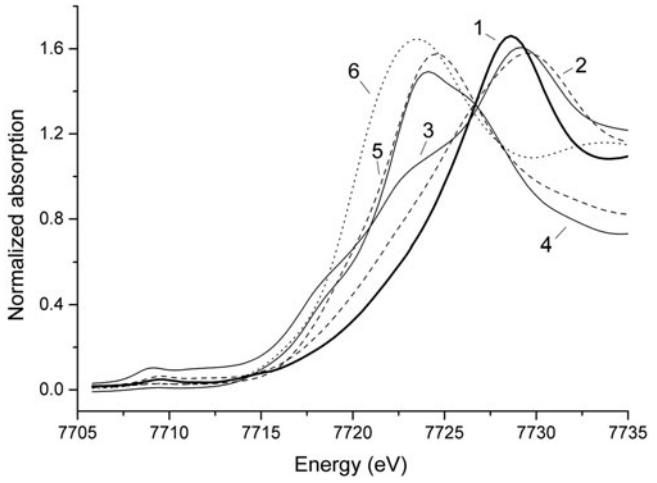

Fig. 6. Co *K*-edge XANES spectrum of kaznakhtite (1) and reference spectra for Co(III) [heterogenite CoOOH from the Democratic Republic of the Congo (2)], Co(II,III) [Co_3O_4 (3)], and Co(II) [$Co(OH)_2$ (4), $CoSO_4$ (5), and $CoCO_3$ (6)] compounds.

Analytical data and standards used are given in Table 1. Contents of other elements with atomic numbers higher than that of beryllium are below detection limits. The empirical formula calculated on the basis of the sum of all metal cations = 8 atoms per formula unit is $(Ni_{5.54}Mg_{0.47}Zn_{0.02})_{\Sigma 6.03}(Co^{3+}_{1.83}Cr_{0.11}Al_{0.03})_{\Sigma 1.97}C_{1.00}O_{2.99}(OH)_{15.84}Cl_{0.16}\cdot 4H_2O$. The simplified formula is $(Ni,Mg)_6(Co^{3+},Cr)_2(CO_3)(OH,Cl)_{16}\cdot 4H_2O$. The ideal formula is $Ni_6Co^{3+}_2(CO_3)(OH)_{16}\cdot 4H_2O$ which requires NiO 51.27, Co_2O_3 18.96, CO_2 5.04, H_2O 24.73, total 100 wt.%.

Kaznakhtite reacts very slowly with cold dilute HCl or HNO_3, however, when the acids are heated, it dissolves within a few seconds with effervescence (CO_2 release).

X-ray diffraction data and crystal structure

Single-crystal X-ray diffraction studies of kaznakhtite could not be carried out because of the earthy nature and tiny size of its crystals. Powder X-ray diffraction data (Table 2) were obtained from a sample containing ~20 wt.% impurity of lizardite-2*H* (Fig. 7). The pattern was recorded in Debye-Scherrer geometry by means of a Rigaku RAXIS Rapid II diffractometer equipped with curved (cylindrical) imaging plate detector (r = 127.4 mm), using Co*K*α radiation (λ = 1.79021 Å) generated by a rotating anode (40 kV and 15 μA) with microfocus optics; exposure time was set to 30 min. The image plate was calibrated against the NIST Si standard. The image-to-profile data processing was performed using *osc2xrd* software (Britvin *et al.*, 2017). Kaznakhtite is trigonal, space group is $R\bar{3}m$, a = 3.0515 (3), c = 23.180 (3) Å, V = 186.93 (4) Å^3 and Z = 3/8. The non-integer Z value is caused by the presentation of the kaznakhtite formula in the form traditional for hydrotalcite-group minerals and accepted by the IMA–CNMNC (Mills *et al.*, 2012a), with 8 metal cations per formula unit. The structural formula of the mineral in a brucite-like sub-cell is $(Ni_{¾}Co^{3+}_{¼})(CO_3)_{1/8}(OH)_2\cdot 0.5H_2O$ with Z = 3. A synthetic analogue of kaznakhtite was described by Mendiboure and Schöllhorn (1986). It has a powder X-ray diffraction pattern similar to that of kaznakhtite (Table 2). The unit-cell parameters of the synthetic phase calculated using the *UNITCELL* program (Holland and Redfern, 1997) are: a = 3.0404(2), c = 23.052(3) Å and V = 184.53(2) Å^3.

The crystal structure of kaznakhtite was refined based on the powder X-ray diffraction pattern (Fig. 7) using full-profile Rietveld refinement. Among several structural models tested, those of reevesite-3*R* $Ni_6Fe^{3+}_2(CO_3)(OH)_{16}\cdot 4H_2O$ (De Waal and Viljoen, 1971; Inorganic Crystal Structure Database (ICSD) #107625) and quintinite-3*R* $Mg_4Al_2(CO_3)(OH)_{12}\cdot 3H_2O$

Table 1. Chemical composition of kaznakhtite (wt.%).

Constituent	Wt.%	Range	S.D.	Reference material
MgO	2.15	1.24–3.58	0.73	Pyrope
NiO	47.40	45.10–50.05	1.68	Ni_2SiO_4
ZnO	0.22	0.00–1.07	0.35	Gahnite
Al_2O_3	0.16	0.00–0.73	0.24	Almandine
Cr_2O_3	0.98	0.30–2.20	0.61	Chromite
Co_2O_3	17.42	15.30–19.07	1.21	Co
Cl	0.63	0.32–0.85	0.15	Vanadinite
$CO_{2calc.}$*	5.05			
$H_2O_{calc.}$*	24.60			
–O=Cl	–0.14			
Total	98.47			

* calculated by stoichiometry
S.D. – standard deviation

https://doi.org/10.1180/mgm.2022.65 Published online by Cambridge University Press

Table 2. Powder X-ray diffraction data (d in Å) for kaznakhtite and its synthetic analogue

Kaznakhtite[a]				Synthetic analogue[b]			
I_{meas}	d_{meas}	I_{calc}	d_{calc}	I_{meas}	d_{meas}	d_{calc}	hkl
100	**7.72**	100	7.73	10	7.63	7.68	003
24	**3.863**	25	3.863	5	3.840	3.842	006
4	**2.630**	3	2.626				101
10	**2.576**	13	2.576	4	2.565	2.567	012
		1	2.575				009
2	2.405	4	2.404	0.5	2.387	2.395	104
6	**2.294**	9	2.296	2	2.285	2.286	015
		1	2.065	0.5	2.075	2.056	107
4	**1.950**	8	1.952	0.5	1.936	1.944	018
		1	1.932				0.0.12
1	1.746	2	1.743	0.5	1.734	1.734	1.0.10
1	1.650	2	1.648	0.5	1.639	1.640	0.1.11
4	**1.526**	2	1.526	2.5	1.521	1.520	110
4	**1.497**	3	1.497	3	1.486	1.491	113
		1	1.478				1.0.13
2	1.419	2	1.419	1	1.415	1.414	$\bar{1}$26
				0.5	1.316	1.314	201
				0.5	1.264	1.264	1.0.16

[a]The calculated pattern was obtained using *the STOE WinXPOW* program, based on unit-cell parameters and atomic coordinates taken from the results of Rietveld refinement. The strongest reflections are marked in boldtype.
[b]Mendiboure and Schöllhorn (1986) (ICDD #33-0429), Debye-Scherrer method, Cu$K\alpha$ radiation, d = 114.6 mm, visual estimation of intensities.

(Zhitova *et al.*, 2016; ICSD #134326) gave the best and almost the same fits between calculated and observed profiles. Because the model reported by Zhitova *et al.* (2016) has the higher symmetry (space group $\bar{R}3m$), it was employed in the final refinement carried out by means of Bruker *TOPAS v.5.0* software. We used a 20-order Chebyshev polynomial to describe the complex shape of the background curve (Fig. 7), because this fit was successfully employed in previous crystallographic works dealing with Rigaku RAXIS image-plate data (e.g. Britvin *et al.*, 2021). Octahedral cation site occupancy was constrained according to the data of electron microprobe analysis. The occupancies of interlayer carbon and oxygen atoms were adjusted to conform charge-balance requirements imposed by the M^{2+}/M^{3+} ratio equal to 3. The coordinates of the oxygen atom in the brucite-like layer and the carbon atom were freely refined. The isotropic displacement parameters were set to be equal for oxygen and carbon atoms. The crystal parameters and details of Rietveld refinement are provided in Table 3, the fractional atomic coordinates and isotropic displacement parameters are given in Table 4, and selected interatomic bond lengths are listed in Table 5. The 3R stacking of the layers in the kaznakhtite structure is illustrated in Fig. 8a. A projection of the interlayer onto {001} is shown in Fig 8b. The oxygen atoms of the CO_3 group are disordered (split) over six symmetrically equivalent positions. Carbonate group positions are populated randomly with an occupancy factor of 0.06. The crystallographic information file has been deposited with the Principal Editor of *Mineralogical Magazine* and is available as Supplementary material (see below).

Discussion

Relationship to other species

Kaznakhtite is the eleventh member of the hydrotalcite group within the hydrotalcite supergroup (Mills *et al.*, 2012a) after desautelsite, droninoite, hydrotalcite, iowaite, meixnerite, pyroaurite, reevesite, stichtite, takovite and woodallite. Most similar chemically to kaznakhtite are reevesite $Ni_6Fe^{3+}_2(CO_3)(OH)_{16}\cdot 4H_2O$ (White *et al.*, 1967; De Waal and Viljoen, 1971) and takovite $Ni_6Al_2(CO_3)(OH)_{16}\cdot 4H_2O$ (Maksimović, 1956; Bish and Brindley, 1977; Mills *et al.*, 2012b); kaznakhtite is their Co^{3+}-dominant analogue.

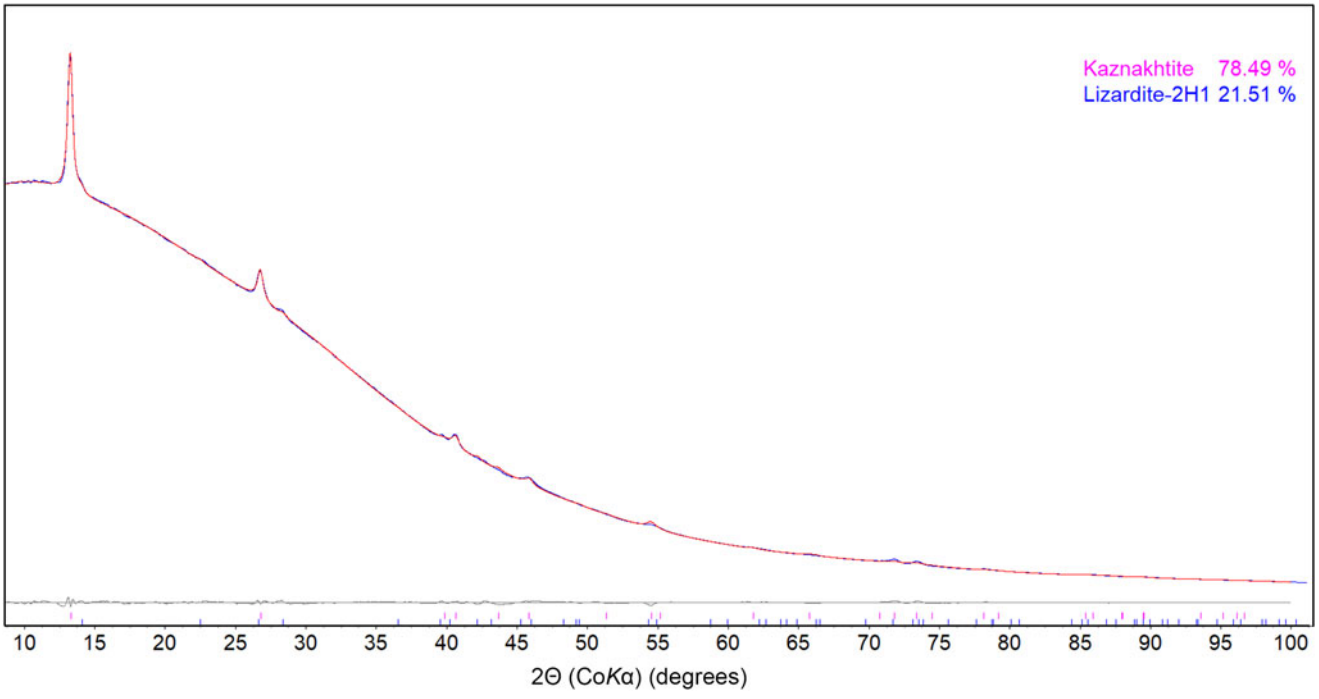

Fig. 7. Rietveld refinement plot of kaznakhtite sample with 22% lizardite-2H_1 impurity.

https://doi.org/10.1180/mgm.2022.65 Published online by Cambridge University Press

Table 3. Crystal parameters and Rietveld refinement details for kaznakhtite.

Crystal data	
Crystal system, space group	Trigonal, $R\bar{3}m$
a (Å)	3.0515(3)
c (Å)	23.180(3)
V (Å^3)	186.93(4)
Z	1
Data collection and refinement	
Diffractometer	Rigaku RAXIS Rapid II (curved image plate)
Radiation	Co$K\alpha_1$ / Co$K\alpha_2$
μ (mm^{-1})	13.036
Exposure time (s)	1800
Calculation step (°)	0.02
$2\theta_{min}$ –$2\theta_{max}$ (°)	10–100
Peak shape description	Modified Pseudo-Voigt
Background subtraction	20-coefficient Chebyshev polynomial
R_p, R_{wp}, R_B (%), GOF	0.30, 0.47, 0.187, 1.88

Table 4. Fractional atomic coordinates and isotropic displacement parameters (B_{iso}, Å^2) for kaznakhtite.

Site	Wykoff position	*x*	*y*	*z*	B_{iso}	Occupancy
*M*1	3*a*	0	0	0	4.8(5)	$Ni_{0.69}Co_{0.23}Mg_{0.06}Cr_{0.01}$
O1	6*c*	⅓	⅔	0.0346(5)	8.1(5)	1
O2 (CO_3)	18*g*	0.103(13)	⅔	⅙	8.1(5)	0.06
C1 (CO_3)	6*c*	0	0	0.165(12)	8.1(5)	0.06
O3 (H_2O)	3*b*	⅓	⅔	⅙	8.1(5)	0.5

Comblainite $Ni_4Co_2^{3+}(CO_3)(OH)_{12}\cdot 3H_2O$ (Piret and Deliens, 1980; Mills *et al.*, 2012a), has the same species-defining elements as kaznakhtite, however, it has a M^{2+}:M^{3+} ratio of 2:1 and, according to the current nomenclature, belongs to the quintinite group within the hydrotalcite supergroup (Mills *et al.*, 2012a). It is well known that the *d*(001) spacing values of hydrotalcite-type layered double hydroxides are dependent on the charge of the brucite-like layer and thus can be used for determination of M^{2+}:M^{3+} ratio (e.g. Wang and Wang, 2007; Sharma *et al.*, 2008; Grover *et al.*, 2010; Zhitova *et al.*, 2016). However, this dependence is not yet applicable for the kaznakhtite/comblainite pair, because the available data are very scarce and controversial (Tables 2 and 6). Therefore, the chemically determined Ni:Co ratio of 3:1 and the trivalent state of Co are the only features which unambiguously distinguish kaznakhtite from other hydrotalcite-group minerals (Table 6).

Song and Moon (1998) reported on the complete solid-solution between reevesite and its unnamed Co^{3+}-dominant analogue from serpentinised ultramafic rocks of the "Buk-site of the Kwangcheon area in Korea" [Buksite, Gwacheon, South Korea]. The material was described as golden yellow fine-grained aggregates replacing early-formed pecoraite–magnetite–millerite–polydymite assemblages during the advanced weathering processes and was studied by electron microprobe analysis, powder X-ray diffraction and IR spectroscopy. The most Co-rich area gave the

Table 5. Selected bond lengths (Å) in the crystal structure of kaznakhtite.

Bond	Length	Notes
*M*1–O1	1.9358(3) × 6	MO_6 octahedron, brucite-like sheet
C1–O2	1.21(2) × 3	CO_3 group

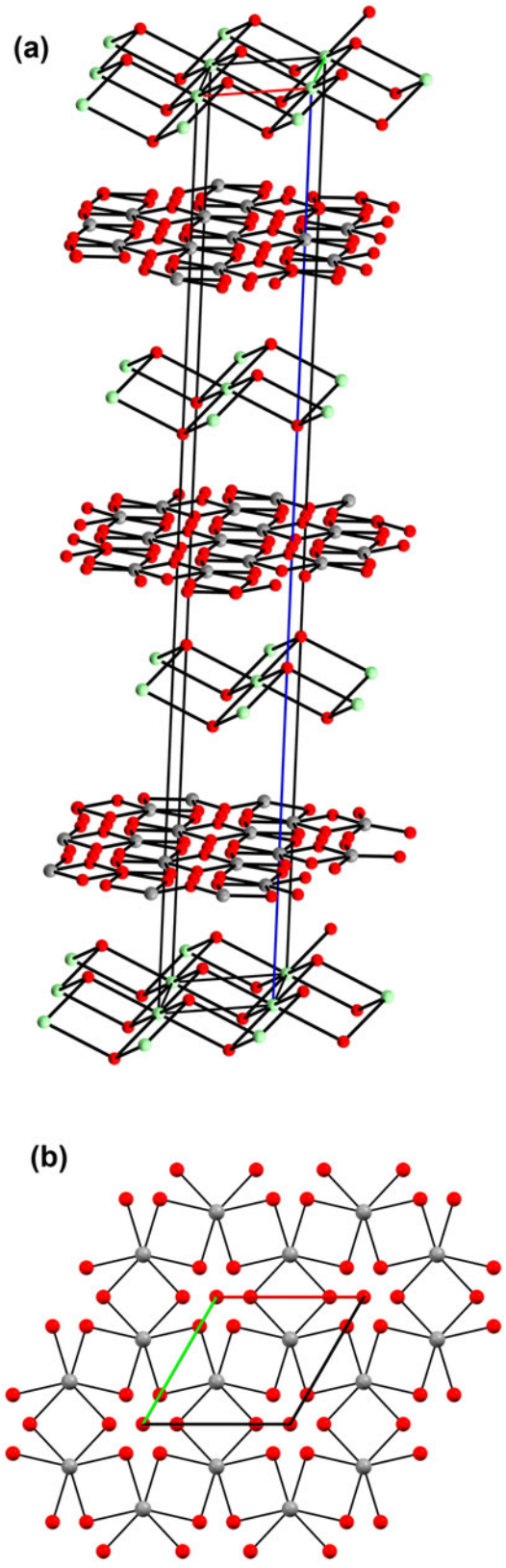

Fig. 8. Crystal structure of kaznakhtite. (a) General view of the structure approximately parallel to the *c* axis. The 3*R* stacking of the interleaving brucite-like and carbonate layers. (b) Projection of carbonate layer onto {001}. The CO_3 group is split into six possible symmetrically equivalent positions. Legend: *M* site (octahedral cations) – pale-green; C – grey; O – red.

https://doi.org/10.1180/mgm.2022.65 Published online by Cambridge University Press

Table 6. Comparative data for kaznakhtite, reevesite, takovite and comblainite.

Mineral	Kaznakhtite	Reevesite	Takovite	Comblainite[a]
Polytype	3*R*	3*R*	3*R*	3*R*
Ideal formula	$Ni_6Co_2^{3+}(CO_3)\ (OH)_{16}{\cdot}4H_2O$	$Ni_6Fe_2^{3+}(CO_3)\ (OH)_{16}{\cdot}4H_2O$	$Ni_6Al_2(CO_3)\ (OH)_{16}{\cdot}4H_2O$	$Ni_4Co_2^{3+}(CO_3)\ (OH)_{12}{\cdot}3H_2O$
Mineral group	Hydrotalcite	Hydrotalcite	Hydrotalcite	Quintinite
Crystal system	Trigonal	Trigonal	Trigonal	Trigonal
Space group	*R3m*	$R\bar{3}$	$R\bar{3}m$	$R\bar{3}m$,*R3m*, $R\bar{3}$, *R*32, *R*3
Unit cell data:				
a (Å)	3.0515	3.079[b]	3.029	3.038
c (Å)	23.18	22.79	22.60	22.79
V (Å^3)	186.93	187.11	179.57	182.16
Z	3/8	3/8	3/8	3/8
Optical data:	Uniaxial (–)	Uniaxial (–)	Uniaxial (–)	Uniaxial (–)
ω	1.672	1.72	1.605	1.690
ε	1.654	1.63	1.598	1.684
Sources:	this paper	White *et al.* (1967); De Waal and Viljoen (1971)	Maksimović (1956); Bish and Brindley (1977); Mills *et al.* (2012b)	Piret and Deliens (1980); Mills *et al.* (2012b)

[a]Piret and Deliens (1980) gave the unit cell of comblainite in rhombohedral setting with the following parameters: $a = 7.796$ Å, $\alpha = 22.47°$, $V = 60.7$ Å^3 and $Z = 1$.
[b]Unit-cell parameters were taken from the structural model reported in the ICSD database (ICSD #107625).

composition close to the kaznakhtite end-member: $(Ni_{6.033}Mg_{0.153})_{\Sigma 6.186}(Co^{3+}_{1.846}Fe^{3+}_{0.055})_{\Sigma 1.901}C_{0.890}S_{0.061}O_3(OH)_{16}{\cdot}4H_2O$. The authors suggested that it is "a new member of the hydrotalcite group", to which "a new mineral name should be given", however, its full description and subsequent submission to the IMA–CNMNC for formal approval never followed. Later, this phase was assigned an unnamed mineral code # UM1998-10-CO:CoHNi (Smith and Nickel, 2007). Taking into consideration the existing data, we are certain that this phase is identical to kaznakhtite. Several synthetic Ni–Co LDH tentatively labelled as 'comblainite' may in fact represent kaznakhtite as well (Zhu and Cao, 2015; Wang and Song, 2017; He *et al.*, 2018).

Remarks on the origin

The origin of kaznakhtite is clearly related to host ultramafic rocks. These rocks are generally enriched in Ni and Co (e.g. Gülaçar and Delaloye, 1976; Herzberg *et al.*, 2016) with the Ni/Co ratio from 2 to 30 (Gülaçar and Delaloye, 1976). These elements are compatible with primary silicates (olivine > pyroxene) and accessory sulfides and (sulfo)arsenides (Herzberg *et al.*, 2016; Hughes *et al.*, 2016). Alteration of primary minerals causes a redistribution of these elements; they can be retained in alteration products or can be remobilised by hydrothermal fluids.

Most likely, kaznakhtite has a supergene origin. For its precipitation, high activities of Ni, Co, and CO_2 are necessary. It could be formed as a result of interaction of CO_2-bearing meteoritic water percolating the ultramafic rocks. Co-bearing heazlewoodite (up to 4 wt.% of Co) found in direct association with kaznakhtite is a possible primary source of nickel and cobalt. They could be also extracted from the host rock. Our chemical analyses show that associated serpentines (lizardite and chrysotile) are Ni-enriched (with NiO content up to 9.1 wt.%). On the other hand, cobalt-rich calcite forms veins ~20 cm thick located directly near the zones of the distribution of stichtite mineralisation in the Kara-Uyuk stream valley (Tatarinov *et al.*, 1985). This is in line with Song and Moon (1998) who proposed the schemes of formation of reevesite by hydroxylation and decomposition of pecoraite (Ni-dominant serpentine). The presence of Co^{3+} in kaznakhtite indicates its formation at strongly oxidising neutral to alkaline conditions (Brookins, 1988). The lenticular shape of the kaznakhtite aggregates suggests rather a local source of Co, e.g. from decomposed Co-bearing sulfide such as heazlewoodite.

The association of kaznakhtite and stichtite is noteworthy – they are isostructural but do not form a solid-solution series. The reason lies in the difference of their origin: stichtite is a Ni- and Co-free hydrothermal mineral at this locality (Zhitova *et al.*, 2020) whereas kaznakhtite is supergene, and they have essentially a different cationic composition.

Supplementary material. To view supplementary material for this article, please visit: https://doi.org/10.1180/mgm.2022.65

Acknowledgements. We acknowledge four anonymous reviewers, Associate and Structure Editor Elena Zhitova and Principal Editor Stuart Mills for valuable comments. The IR spectroscopy investigation was carried out in accordance with the state task of the Russian Federation, state registration No. AAAA-A19-119092390076-7. RŠ thanks the MUNI/A/1570/2021 research project of Masaryk University for support. The X-ray diffraction study was carried out using the facilities of the Centre for X-ray Diffraction Studies, Saint-Petersburg State University.

Competing interests. The authors declare none.

References

Bindi L., Christy A.G., Mills S.J., Ciriotti M.E. and Bittarello E. (2015) New compositional and structural data validate the status of jamborite. *The Canadian Mineralogist*, **53**, 791–802.

Bish D.L. and Brindley G.W. (1977) A reinvestigation of takovite, a nickel aluminum hydroxy-carbonate of the pyroaurite group. *American Mineralogist*, **62**, 458–464.

Britvin S.N. (2008) Structural diversity of layered double hydroxides. Pp 123–128 in: *Minerals as Advanced Materials II* (S.V. Krivovichev, editor). Springer-Verlag, Berlin–Heidelberg.

Britvin S.N., Dolivo-Dobrovolsky D.V. and Krzhizhanovskaya M.G. (2017) Software for processing the X-ray powder diffraction data obtained from the curved image plate detector of Rigaku RAXIS Rapid II diffractometer. *Zapiski Rossiiskogo Mineralogicheskogo Obshchestva*, **146**(3), 104–107 [in Russian].

Britvin S.N., Krzhizhanovskaya M.G., Zolotarev A.A., Gorelova L.A., Obolonskaya E.V., Vlasenko N.S., Shilovskikh V.V. and Murashko M.N. (2021) Crystal chemistry of schreibersite, $(Fe,Ni)_3P$. *American Mineralogist*, **106**, 1520–1529.

Brookins D.G. (1988) *Eh-pH Diagrams for Geochemistry*. Springer Science & Business Media. 176 pp.

De Waal S.A. and Viljoen E.A. (1971) Nickel minerals from Barberton, South Africa: IV. Reevesite, a member of the hydrotalcite group. *American Mineralogist*, **56**, 1077–1081.

Evans D.G. and Slade R.C.T. (2006) Structural aspects of layered double hydroxides. Pp. 1–87 in: *Layered Double Hydroxides* (X. Duan and D.G. Evans, editors). Structure, Vol. **119**. Springer, Berlin–Heidelberg.

Grover K., Komarneni S. and Katsuki H. (2010) Synthetic hydrotalcite-type and hydrocalumite-type layered double hydroxides for arsenate uptake. *Applied Clay Science*, **48**, 631–637.

Gülaçar O.F. and Delaloye M. (1976) Geochemistry of nickel, cobalt and copper in alpine-type ultramafic rocks. *Chemical Geology*, **17**, 269–280.

He P., Zhang Q., Huang Q., Huang B. and Chen T. (2018) Vertically-oriented graphene nanosheet as nano-bridge for pseudocapacitive electrode with ultrahigh electrochemical stability. *RSC Advances*, **8**, 13891–13897.

Herzberg C., Vidito C. and Starkey, N.A. (2016) Nickel–cobalt contents of olivine record origins of mantle peridotite and related rocks. *American Mineralogist*, **101**, 1952–1966.

Holland T.J.B. and Redfern S.A.T. (1997) UNITCELL: a nonlinear least-squares program for cell-parameter refinement and implementing regression and deletion diagnostics. *Journal of Applied Crystallography*, **30**, 84.

Hughes H.S., McDonald I., Faithfull J.W., Upton B.G. and Loocke M. (2016) Cobalt and precious metals in sulphides of peridotite xenoliths and inferences concerning their distribution according to geodynamic environment: a case study from the Scottish lithospheric mantle. *Lithos*, **240**, 202–227.

Karpenko V.Y., Zhitova E.S., Pautov L.A., Agakhanov A.A., Siidra O.I., Krzhizhanovskaya M.G., Rassulov V.A. and Bocharov V.N. (2020) Akopovaite, $Li_2Al_4(OH)_{12}(CO_3)(H_2O)_3$, a new Li member of the hydrotalcite supergroup from Turkestan Range, Kyrgyzstan. *Mineralogical Magazine*, **84**, 301–311.

Kasatkin A.V., Britvin S.N., Krzhizhanovskaya M.G., Chukanov N.V., Škoda R., Göttlicher J., Belakovskiy D.I., Pekov I.V. and Levitskiy V.V. (2021): Kaznakhtite, IMA 2021-056. CNMNC Newsletter 63. *Mineralogical Magazine*, **85**, https://doi.org.10.1180/mgm.2021.74

Krivovichev S.V., Yakovenchuk V.N., Zhitova E.S. (2012) Natural double layered hydroxides: structure, chemistry, and information storage capacity. Pp 87–91 in: *Minerals as Advanced Materials II* (S.V. Krivovichev, editor). Springer–Verlag, Berlin–Heidelberg.

Kuznetsov V.A. (1958) Age of the ultrabasic intrusions of the Gornyy Altai. *Izvestiya of the Academy of Sciences of the U.S.S.R. Geologic series*, **4**, 66–74.

Maksimović Z. (1956) Takovite, hydrous nickel aluminate, a new mineral. *Zapisnici Srpskog Geoloskog Drustva*, 219–224.

Mandarino J.A. (1981) The Gladstone–Dale relationship. IV. The compatibility concept and its application. *The Canadian Mineralogist*, **19**, 441–450.

Mendiboure A. and Schöllhorn R. (1986) Formation and anion exchange reactions of layered transition metal hydroxides $[Ni_{1-x}M_x](OH)_2(CO_3)_{x/2}(H_2O)_z$(M = Fe,Co). *Revue de Chimie minérale*, **23**, 819–827.

Merlet C. (1994) An accurate computer correction program for quantitative electron probe microanalysis. *Microchimica Acta*, **114/115**, 363–376.

Mills S.J., Christy A.G., Génin J-M.R., Kameda T. and Colombo F. (2012a) Nomenclature of the hydrotalcite supergroup: natural layered double hydroxides. *Mineralogical Magazine*, **76**, 1289–1336.

Mills S.J., Whitfield P.S., Kampf A.R., Wilson S.A., Dipple G.M., Raudsepp M. and Favreau G. (2012b) Contribution to the crystallography of hydrotalcites: the crystal structures of woodallite and takovite. *Journal of Geosciences*, **58**, 273–279.

Piret P. and Deliens M. (1980) La comblainite, $(Ni_x^{2+}Co_{1-x}^{3+})(OH)_2(CO_3)_{(1-x)/2}\cdot yH_2O$, nouveau minéral du groupe de la pyroaurite. *Bulletin de Minéralogie*, **103**, 113–117.

Ravel B. and Newville M. (2005) ATHENA, ARTEMIS, HEPHAESTUS: Data analysis for X-ray absorption spectroscopy using IFEFFIT. *Journal of Synchrotron Radiation*, **12**, 537–541.

Rives V. (editor) (2001) *Layered Double Hydroxides: Present And Future*. Nova Science Publishers, Inc, New York, USA, 493 pp.

Rychkov V.M. and Rychkova S.I. (2015) On the findings of stichtite (barbertonite) and talc in Gorny Altai. *Prirodnye resoursy Gornogo Altaya* [Natural Resources of Gorny Altai], **18**, 27–31.

Sharma S.K., Parikh P.A. and Jasra R.V. (2008) Eco-friendly synthesis of jasminaldehyde by condensation of 1-heptanal with benzaldehyde using hydrotalcite as a solid base catalyst. *Journal of Molecular Catalysis A*, **286**, 55–62.

Smith D.G.W. and Nickel E.H. (2007) A system for codification for unnamed minerals: report of the Subcommittee for Unnamed Minerals of the IMA Commission on New Minerals, Nomenclature and Classification. *The Canadian Mineralogist*, **45**, 983–1055.

Song Y. and Moon H.-S. (1998) Additional data on reevesite and its Co-analogue, as a new member of the hydrotalcite group. *Clay Minerals*, **33**, 285–296.

Tatarinov A.V., Sapozhnikov A.N., Prokudin S.G. and Frolova L.P. (1985) Stichtite in serpentinites of the Terektinsky Ridge (Altay). *Zapiski Vserossijskogo Mineralogicheskogo Obshchestva*, **114**, 575–581 [in Russian].

Wang X. and Song T. (2017) Buckypaper templating Ni-Co hydroxide nanosheets film with stimuliresponsive properties. *Materials Letters*, **200**, 113–117.

Wang S.-L. and Wang P.-C. (2007) In situ XRD and ATR-FTIR study on the molecular orientation of interlayer nitrate in Mg/Al-layered double hydroxides in water. *Colloids and Surfaces A*, **292**, 131–138.

White J.S. Jr, Henderson E.P. and Mason B. (1967) Secondary minerals produced by weathering of the Wolf Creek meteorite. *American Mineralogist*, **52**, 1190–1197.

Yang H., Gibbs R.B., Schwenk C., Xie X., Gu X., Downs R.T. and Evans S.H. (2021) Liudongshengite, $Zn_4Cr_2(OH)_{12}(CO_3)\cdot 3H_2O$, a new mineral of the hydrotalcite supergroup, from the 79 mine, Gila County, Arizona, USA. *The Canadian Mineralogist*, **59**, 763–769.

Zhitova E.S., Krivovichev S.V., Pekov I.V., Yakovenchuk V.N. and Pakhomovsky Ya.A. (2016) Correlation between the *d*-value and the M^{2+}:M^{3+} cation ratio in Mg–Al–CO_3 layered double hydroxides. *Applied Clay Science*, **130**, 2–11.

Zhitova E.S., Pekov I.V., Chaikovskiy I.I., Chirkova E.P., Yapaskurt V.O., Bychkova Y.V., Belakovskiy D.I., Chukanov N.V., Zubkova N.V., Krivovichev S.V. and Bocharov V.N. (2019) Dritsite, $Li_2Al_4(OH)_{12}Cl_2\cdot 3H_2O$, a new gibbsite-based hydrotalcite supergroup mineral. *Minerals*, **9**, 492.

Zhitova E.S., Pekov I.V., Chukanov N.V., Yapaskurt V.O. and Bocharov S.N. (2020) Minerals of the system stichtite-pyroaurite-iowaite-woodallite from serpentinites of the Terekta Ridge (Gorny Altai, Russia). *Russian Geology and Geophysics*, **61**, 36–46.

Zhitova E., Chukanov N., Jonsson E., Pekov I., Belakovskiy D., Vigasina M., Zubkova N., Van K. and Britvin S. (2021) Erssonite, $CaMg_7Fe_2^{3+}(OH)_{18}(SO_4)_2\cdot 12H_2O$, a new hydrotalcite-supergroup mineral from Långban, Sweden. *Mineralogical Magazine*, **85**, 817–826.

Zhu Y. and Cao C. (2015) A simple synthesis of two-dimensional ultrathin nickel cobaltite nanosheets for electrochemical lithium storage. *Electrochimica Acta*, **176**, 141–148.

https://doi.org/10.1180/mgm.2022.65 Published online by Cambridge University Press